

See discussions, stats, and author profiles for this publication at: <https://www.researchgate.net/publication/263953165>

Pressure Drop and Liquid Distribution in a Venturi Scrubber: Experimental Data and CFD Simulation

ARTICLE *in* INDUSTRIAL & ENGINEERING CHEMISTRY RESEARCH · JUNE 2012

Impact Factor: 2.59 · DOI: 10.1021/ie202871q

CITATIONS

2

READS

37

4 AUTHORS, INCLUDING:



V. G. Guerra

Universidade Federal de São Carlos

13 PUBLICATIONS 19 CITATIONS

[SEE PROFILE](#)



Rodrigo Béttega

Universidade Federal de São Carlos

17 PUBLICATIONS 68 CITATIONS

[SEE PROFILE](#)

Pressure Drop and Liquid Distribution in a Venturi Scrubber: Experimental Data and CFD Simulation

Vádila G. Guerra,[†] Rodrigo Béttega,[‡] José A. S. Gonçalves,^{*,†} and José R. Coury[†]

[†]Department of Chemical Engineering, Federal University of São Carlos, Via Washington Luiz, Km 235, 13565-905, São Carlos—SP, Brazil

[‡]School of Chemical Engineering, Federal University of Uberlândia, R. 770, Av. João Naves de Ávila 2121, 38408-100, Uberlândia—MG, Brazil

ABSTRACT: Venturi scrubbers are widely used to control industrial emissions, because of their high efficiency in the removal of particles from gases. To correctly size and design these equipments, detailed information on the fluid dynamics is very important. The purpose of this article is to study, both experimentally and through CFD simulations, the fluid dynamics of the gas and liquid phases in the core of the throat of a rectangular Venturi scrubber under different experimental conditions. The variables studied were the pressure and the volumetric fraction of each phase. The standard $\kappa-\epsilon$ turbulence model and the volume of fluid (VOF) multiphase model, as implemented in the ANSYS Fluent 12.0 software, were employed. Liquid distribution inside the throat of the Venturi was studied experimentally, using optical imaging techniques. The results indicate that the model and numerical procedures were able to describe both the pressure drop profile and the liquid jet formation and trajectory successfully. The results suggest that, for the same gas and liquid flow rates, the number of liquid injection orifices does not affect the pressure drop, but affects significantly the liquid fraction distribution profile inside the equipment.

1. INTRODUCTION

Venturi scrubbers are widely used to control industrial emissions, because of their high efficiency in collecting particles from dust-laden gases. These equipments use liquid to collect the particles.

Venturi scrubbers consist basically of three parts: the convergent section, the constriction called throat, and the divergent section. The liquid is usually injected in the form of jets through orifices located on the throat. In contact with high-velocity gas, the jets are atomized forming numerous droplets, which are responsible for collecting the particles. The energy needed to atomize the liquid and accelerate it comes from the high-velocity gas, because of a momentum exchange between the gaseous and liquid phases. The loss of mechanical energy of the gas stream is reflected in the pressure drop of the system. From the economic point of view, it is critical to consider the loss of mechanical energy.

Computational fluid dynamics (CFD) has been gaining highlights in recent years for predicting fluid dynamic behavior of a wide range of industrial equipments. In particular, studies on multiphase systems represent bigger challenges in terms of mathematical modeling and numerical simulation, and are the subject of recent studies by various researchers. These studies show that CFD can be used to predict fluid dynamic behavior of multiphase flow of different types.^{1–7} Studies that predict the fluid dynamic behavior of Venturi scrubbers range from simple models, such as that proposed by Calvert,⁸ designed to predict pressure drop in Venturi scrubbers, to recent phenomenological models in CFD, such as studies done by Ananthanarayanan and Viswanathan,⁹ Pak and Chang,³ and Ahmadvand and Talaie.⁴

Gonçalves et al.² summarized and evaluated the most important models and correlations available in the literature to estimate the pressure drop in Venturi scrubbers by comparing the results predicted by these models^{8,10–14} with experimental

data from Venturi scrubbers of different sizes and experimental conditions. Of the models evaluated, that proposed by Azzopardi et al.¹⁴ was the only one that demonstrated good predictions for the entire range of variables studied.

More recently, Sun and Azzopardi¹⁵ evaluated a full boundary layer model, following the model previously proposed by Azzopardi et al.,¹⁴ and checked its performance in predicting data for a system operating under high pressure. The model modified by the authors showed good results. Rahimi et al.¹⁶ developed a single-directional descriptive mathematical model to predict the pressure drop in Venturi scrubbers, particularly considering the equations of conservation of mass and energy. The authors showed that the occurrence of heat transfer between the phases contributes to reducing the pressure drop in the equipment.

In addition to pressure drop, the particle collection efficiency is the other important design parameter, and this is largely influenced by the liquid distribution inside the equipment.¹⁷ The distribution of liquid in Venturi scrubbers is usually not uniform and depends on the number and position of the injection orifices on the scrubber throat, as well as the liquid and gas flow rates.¹ A uniform dispersion of liquid can increase the equipment's collection performance, since it makes the contact between the particles and a collector droplet more likely.^{9,18,19} Some mathematical models for Venturi scrubbers incorporate droplet dispersion to predict the efficiency of collection.^{3,9,19} When the liquid is injected via orifices, the initial liquid distribution is related to the jet penetration.²⁰ In the existing

Received: December 7, 2011

Revised: May 10, 2012

Accepted: May 16, 2012

Published: May 16, 2012

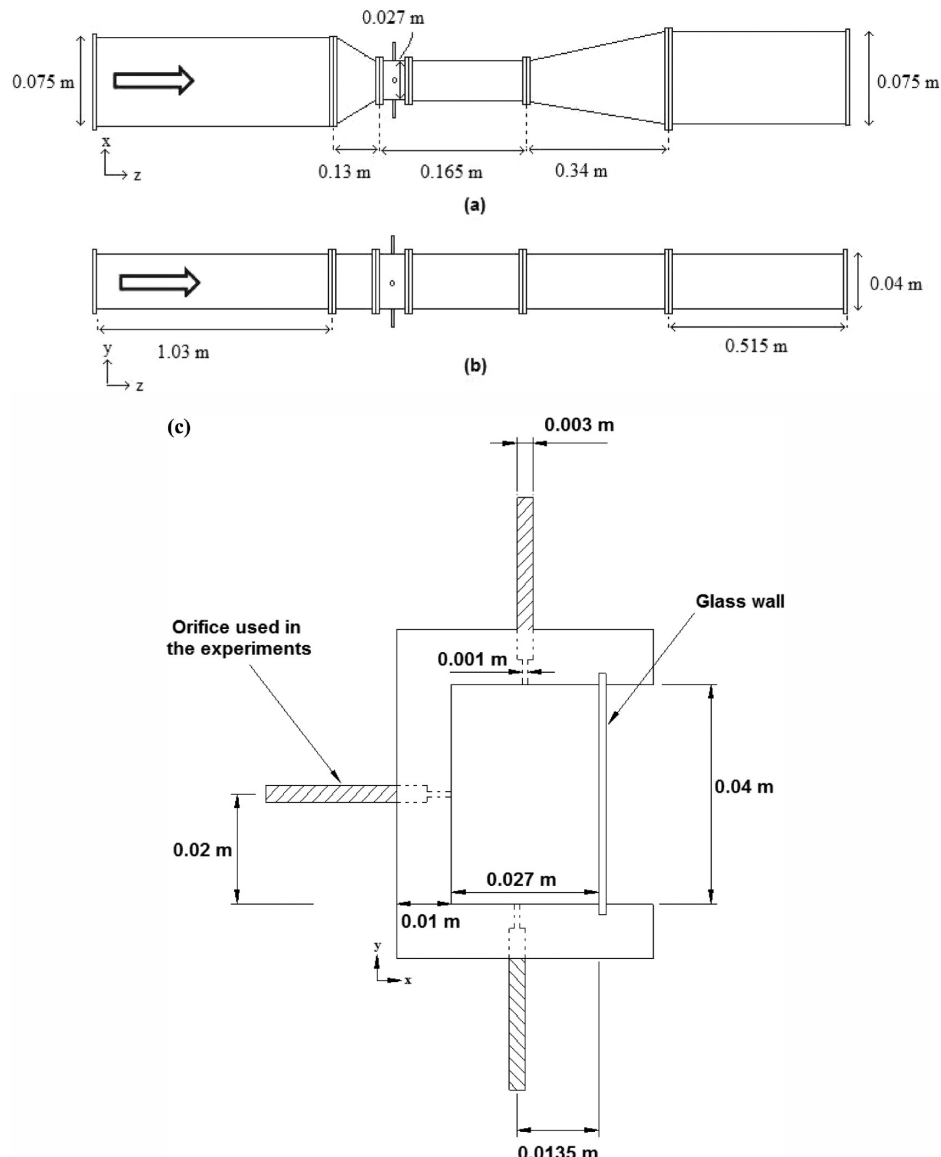


Figure 1. Principal dimensions of the equipment: (a) front view, (b) side view, and (c) details of the throat.

literature, there is a scarcity of studies on droplet dispersion in Venturi scrubbers with varying numbers of orifices for liquid injection.^{9,20,21}

Two generic approaches (Eulerian–Eulerian and Eulerian–Lagrangian) have been extensively used for modeling two-phase flow with a particulate phase. When the particulate phase is described by a Lagrangian approach, the velocity, mass, and temperature of each representative particle is calculated and stored. By contrast, in the Eulerian–Eulerian approach, the particulate phase is considered a second fluid which behaves like a continuum. Although only average properties for the particulate phase can be computed in the Eulerian–Eulerian (also called two-fluid) approach demands much less computational power. Both approaches have been used on the modeling of Venturi scrubbers. The Lagrangian approach has been employed by Pak and Chang,³ while the two-fluid approach by Gonçalves et al.,¹ Ahmadvand and Talaie,³ and Ananthanarayanan and Viswanathan.⁹ A common feature in all these works, regardless of the approach used, is that the liquid phase is modeled as consisting only of droplets that are dispersed throughout the equipment. The liquid jet is, at most, modeled separately,¹ only to

provide source points for the droplets. The present work, however, is aimed at using a single model to describe the liquid phase (jet injection and liquid dispersion). With this purpose in mind, only the Eulerian–Eulerian approach was viable.

Among the several variants of the Eulerian–Eulerian approach, the volume of fluid (VOF) method presented itself as an interesting possibility, because it has been typically applied to track liquid/gas interfaces, such as in the prediction of jet breakup.²² Moreover, in the particular case of Venturi scrubbers, where inflow boundaries are distinct for each fluid and the solution is independent from the initial conditions, the VOF method could be applied to a steady-state simulation. The VOF method, however, has not been usually applied to track the dispersion of small droplets in a gas, and it remained to be shown (as it is done in this paper) if it would be capable of successfully doing that under typical Venturi scrubber conditions.

In the present article, experimental data on pressure drop and liquid distribution inside of a Venturi scrubber with a rectangular cross section were compared with the results predicted by a CFD simulation, obtained from the implementation of an Eulerian–Eulerian volume of fluid (VOF) model. In the simulations, a

three-dimensional geometry was adopted to make it possible to simulate different configurations of injection orifices.

2. EXPERIMENTAL PROCEDURE

All the experimental tests were taken in with a rectangular Venturi scrubber built in acrylic modules with a $0.040\text{ m} \times 0.027\text{ m}$ throat rectangular cross section. The main dimensions of the equipment are shown in Figure 1. A positive displacement pump transported water from a reservoir to the scrubber injection orifices located on the throat, passing first through a rotameter to measure the flow rate. The equipment throat had a front wall of glass, to facilitate the capture of photographic images of the liquid jets. The other walls were made of acrylic and painted black to increase contrast and improve image quality. Except for the glass wall, there was an injection orifice on each wall. An injection orifice on the glass wall was not included in order not to obstruct the visualization of the other liquid jets as well as the distribution of liquid inside the throat. Thus, the throat has a total of three injection orifices, each of them with a 0.001 m diameter, as can be observed in Figure 1c.

Four gas flow rates were used in the experiments, corresponding to superficial throat gas velocities of 59, 64, 69, and 74 m/s . The number of orifices injecting liquid varied from one to three.

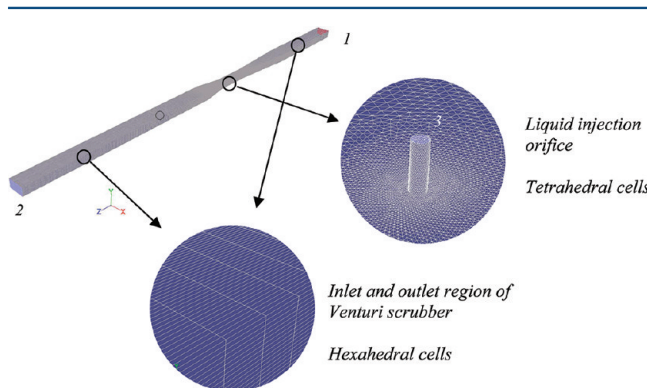


Figure 2. Computational mesh used.

Equation 1 shows the correlation proposed by Viswanathan et al.²³ to determine jet penetration in Venturi scrubbers:

$$I^{**} = 0.1145 \left(\frac{\rho_l}{\rho_g} \right) \left(\frac{V_l}{V_g} \right) d_o \quad (1)$$

To obtain the necessary liquid flow rate from the desired jet penetration, the correlation proposed by Viswanathan et al.²³ was manipulated. Thus, the term Q_l , which represents the total liquid flow rate, for the injection of liquid into more than one orifice is given by eq 2:

$$Q_l = \frac{I^{**} Q_g \rho_g d_o N_o}{0.1458 \rho_l A_{th}} \quad (2)$$

The liquid flow rate (Q_l) was allowed to vary, but the relative jet penetration (I^{**}/D_h ratio, where D_h is the throat hydraulic diameter ($D_h = 0.032\text{ m}$)) was fixed at four values: 0.2, 0.3, 0.4, and 0.5. The total liquid flow rate varied from $2 \times 10^{-6}\text{ m}^3/\text{s}$ to $3 \times 10^{-5}\text{ m}^3/\text{s}$.

Static pressure was measured at 15 different pressure tappings throughout the equipment walls. An electronic manometer was used to take these measurements. This setup ensured that pressure readings could be obtained without any interference on the flow.

Images of the liquid jet and liquid distribution in the throat of the Venturi scrubber were taken using a Sony video camera, Model DCR-DVD 403 with a resolution of 3 megapixels and shuttering velocity of $250\text{ }\mu\text{s} \pm 5\text{ }\mu\text{s}$. The throat was illuminated with an electronic flash circuit using 100 white leds ($\sim 10\,000\text{ cd}$ in total), which could be configured to operate $20\text{ }\mu\text{s}$ on and $1000\text{ }\mu\text{s}$ off per period and was monitored by an oscilloscope.

Table 1. Values for Experimental and Simulated Pressure Drop without Liquid Injection

V_g (m/s)	ΔP_{exp} (Pa)	ΔP_{simul} (Pa)	deviation (%)
59	666.61	665.41	0.18
64	799.93	755.28	5.60
69	933.25	923.40	1.05
74	1010.45	980.87	2.93

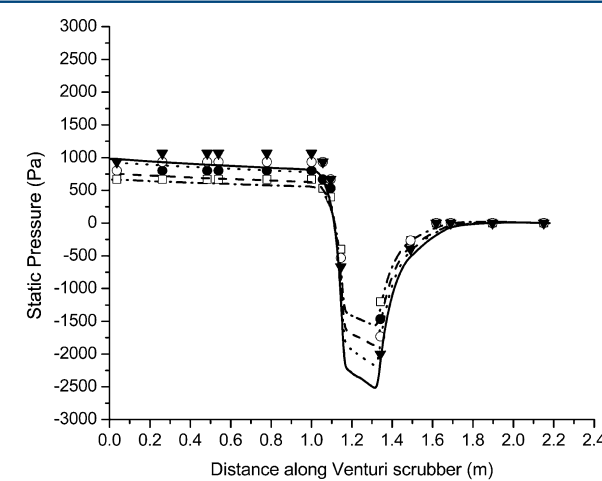


Figure 3. Measurement of experimental and simulated static pressure along the Venturi scrubber without liquid injection.

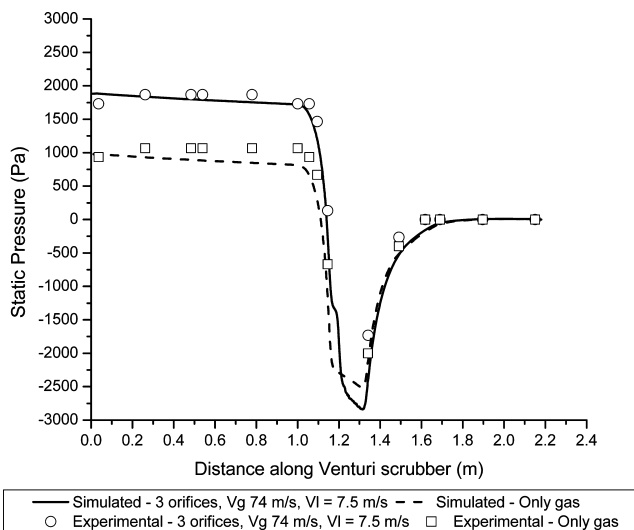


Figure 4. Experimental and simulated measurements of static pressure $V_g = 74 \text{ m/s}$, without liquid injection and with liquid injection through three orifices and $V_l = 7.5 \text{ m/s}$ ($\Gamma^{**}/D_h = 0.3$).

The flash was located on the top part of the throat. The camcorder was placed as close to the glass wall as possible. The distance between the camcorder and the center of the channel was 2 cm.²⁴

3. MODELING AND NUMERICAL PROCEDURE

This work used the front-tracking method to describe the behavior of the two-phase gas–liquid flow. The mathematical modeling is based on an Eulerian approach to describe the field of pressures and the fluid velocity, where a single equation for the conservation of momentum (eq 3) is applied to the domain and the resulting velocity and pressure fields are shared among the phases.

$$\frac{\partial}{\partial t}(\rho \vec{v}) + \nabla \cdot (\rho \vec{v} \vec{v}) = -\nabla p + \nabla \cdot [\mu(\nabla \vec{v} + \nabla \vec{v}^T)] + \rho \vec{g} \quad (3)$$

In eq 3, \vec{v} represents the velocity vector and μ and ρ are the viscosity and density of the mixture and, therefore, are dependent on the volume fraction of each phase in a computational cell.

The identification of the different fluids is done by a marker inserted into the system, which is advected by the flow. In a general way, the interface capture methods are based on a fixed mesh and use an additional marker function to identify the position of the interface. Among other things, the interface capture VOF (volume of fluid) method adopted for this work has the advantage of simplicity and the ability to solve these problems.

The VOF approach is based on the fact that the flow phases are not interpenetrable. For each phase in the model, a variable representing its volumetric fraction in the cell of the system is added.

Identifying the interface among the flow phases for the problem described in this article is accomplished by solving a continuity equation for the volumetric fraction of the liquid phase present in the gas–liquid flow. For the liquid phase (α_l), the equation for the conservation of the volumetric fraction is presented in eq 4, where

$$\frac{\partial \alpha_l}{\partial t} = \nabla \cdot (\alpha_l \vec{v}_l) \quad (4)$$

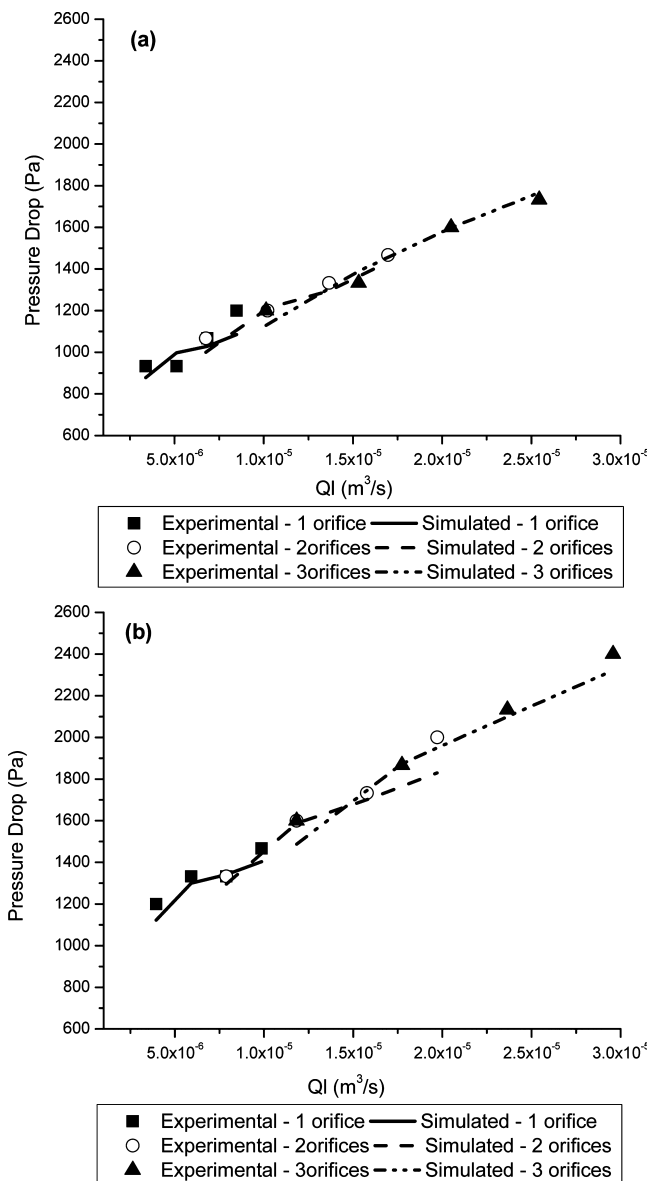


Figure 5. Effect of the liquid flow rate on the pressure drop: (a) $V_g = 64 \text{ m/s}$ and (b) $V_g = 74 \text{ m/s}$.

Equation 4 is valid for incompressible fluids with no mass transfer between the phases and also considering the nonexistence of mass source terms. In a general way, cells with a volumetric fraction of fluid between 0 and 1 contain a flow interface. In this work, the simulations were done in the steady-state regime, meaning that the transient term in eq 4 was equal to zero.

In this work, eq 4 was solved for the liquid phase. For the gas (primary) phase, the volumetric fraction is calculated considering that the sum of the fractions for all phases in the volume must be equal to the unit. To solve eq 4 the implicit formulation was adopted. More information on the method of implicit discretization, as well as the VOF approach, can be found in the work of Hirt and Nichols²⁵ and FLUENT.²⁶

System turbulence was solved according to the $k-\epsilon$ RNG model. This model is the result of adapting Navier–Stokes equations, using statistical techniques. The RNG has greater representativeness and reliability, compared to the standard $k-\epsilon$

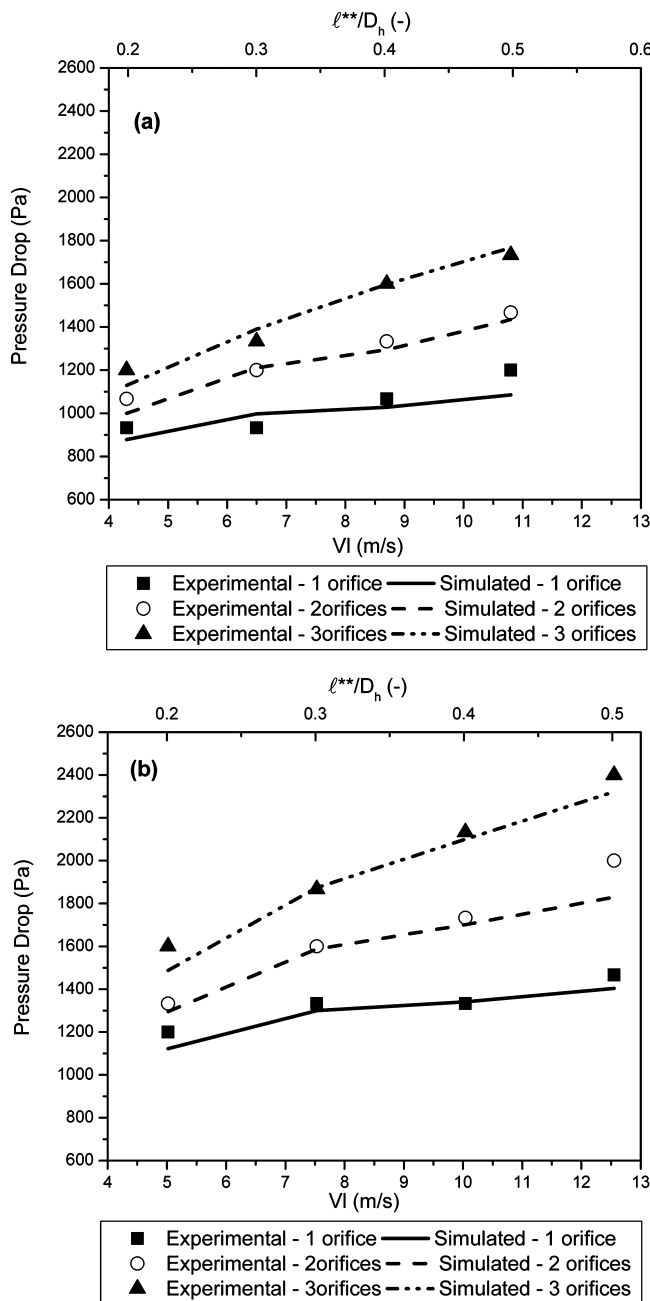


Figure 6. Effect of the liquid velocity on the pressure drop: (a) $V_g = 64 \text{ m/s}$ and (b) $V_g = 74 \text{ m/s}$.

model for a broader range of flows. More information on the turbulence model adopted here can be found in Orzag et al.²⁷

A three-dimensional computational domain was used to solve the fluid dynamics of this problem. The three-dimensional

geometry was adopted in virtue of the need to vary the number of injections in the equipment throat in order to make possible a numerical assessment of their effects on the fluid dynamic behavior of the system.

The computational mesh was developed using the software GAMBIT 2.4.6, respecting the dimensions and other geometric features of the equipment, as shown in Figure 1. The computational domain includes the exit and entry ducts of the equipment as well, avoiding unreal turbulence in the liquid jet due to entrance effects. By extending the computational domain in this way, the flow is fully developed when it reaches the region of interest. Figure 2 illustrates the computer mesh adopted in this work.

Preliminary tests done using different mesh sizes and configurations indicated the mesh features and degree of refinement needed for achieving a stable solution with reasonable computational costs. The hybrid mesh adopted in this work had 1 178 610 cells, with 2 540 298 faces and 333 383 nodes. Hexahedral cells were used in the entry and exit regions of the equipment and tetrahedral cells in the throat and liquid injection orifices. The mesh was refined near the liquid injection orifices (Figure 2).

The boundary conditions applied to the solution of the model were as follows (see Figure 2):

- Air entry (point 1): prescribed velocity at the face and volumetric fraction of the liquid null;
- Exit of air and liquid (point 2): prescribed atmospheric pressure on the face;
- Liquid injection (point 3): prescribed velocity at the face and volumetric fraction of air null;
- Equipment walls: nonslippery condition for both fluids.

The numerical solution to the problem was accomplished using the commercial package CFD ANSYS FLUENT 12.0, through the VOF method (Hirt and Nichols²⁵) applied to the solution of the incompressible and isothermal two-phase flow. The pressure-velocity coupling was solved using the phase-coupled SIMPLE algorithm.²⁸ Second-degree UPWIND discretizations for the momentum and turbulence equations were used. This discretization scheme is able to avoid false numerical diffusion, when compared with first-order schemes, with lower computational costs in comparison with higher-order schemes. Gravitational effects were ignored in the simulations. The convergence criteria for all problem variables were maintained at 10^{-4} , with relaxation parameters in the range of 0.2–0.4.

4. RESULTS AND DISCUSSION

4.1. Pressure Drop without Liquid Infection. Figure 3 presents experimental and simulated data on static pressure for different gas velocities without liquid injection. The simulated results correspond to the pressure values on the equipment walls, corresponding to the positions of the experimental measurements. It is possible to observe the classic behavior of the Venturi

Table 2. Values for Pressure Drop for Different Liquid Velocities and $V_g = 64 \text{ m/s}$

V_l (m/s)	ℓ^{**}/D_h	One Orifice			Two Orifices			Three Orifices		
		ΔP_{exp} (Pa)	ΔP_{simul} (Pa)	deviation (%)	ΔP_{exp} (Pa)	ΔP_{simul} (Pa)	deviation (%)	ΔP_{exp} (Pa)	ΔP_{simul} (Pa)	deviation (%)
4.3	0.2	933.25	878.04	5.92	1066.58	1000.56	6.19	1199.90	1129.18	5.89
6.5	0.3	933.25	997.67	6.90	1199.89	1211.11	0.94	1333.2	1390	4.26
8.7	0.4	1066.57	1028.57	3.56	1333.20	1293.94	2.94	1599.86	1597.22	0.17
10.8	0.5	1199.89	1085.45	9.54	1466.54	1434.63	2.18	1733.19	1767.07	1.96

Table 3. Values for Pressure Drop for Different Liquid Velocities and $V_g = 74 \text{ m/s}$

$V_l (\text{m/s})$	I^{**}/D_h	One Orifice			Two Orifices			Three Orifices		
		$\Delta P_{\text{exp}} (\text{Pa})$	$\Delta P_{\text{simul}} (\text{Pa})$	deviation (%)	$\Delta P_{\text{exp}} (\text{Pa})$	$\Delta P_{\text{simul}} (\text{Pa})$	deviation (%)	$\Delta P_{\text{exp}} (\text{Pa})$	$\Delta P_{\text{simul}} (\text{Pa})$	deviation (%)
5.0	0.2	1199.89	1123.12	6.40	1333.22	1295.06	2.86	1599.86	1487.68	7.01
7.5	0.3	1333.32	1299.51	2.53	1599.90	1587.22	0.79	1866.51	1873.44	0.37
10.0	0.4	1333.32	1340.43	0.53	1733.19	1701.12	1.85	2133.15	2099.47	1.58
12.5	0.5	1466.51	1402.95	4.33	1999.83	1829.22	8.53	2399.80	2321.62	3.26

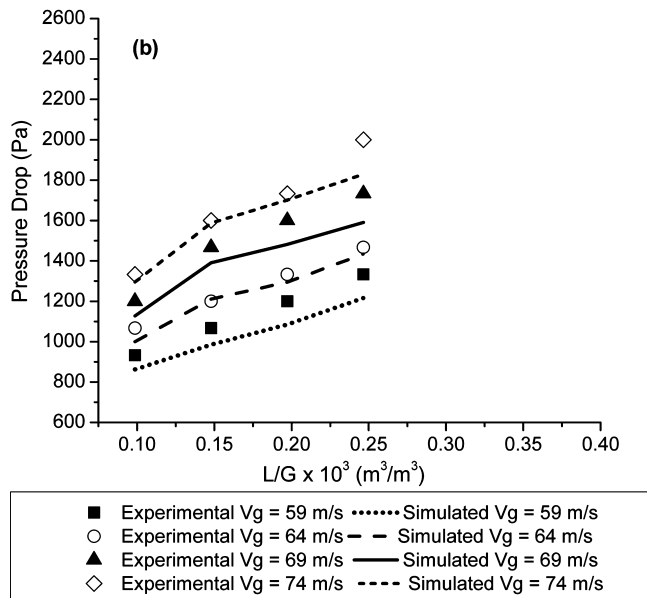
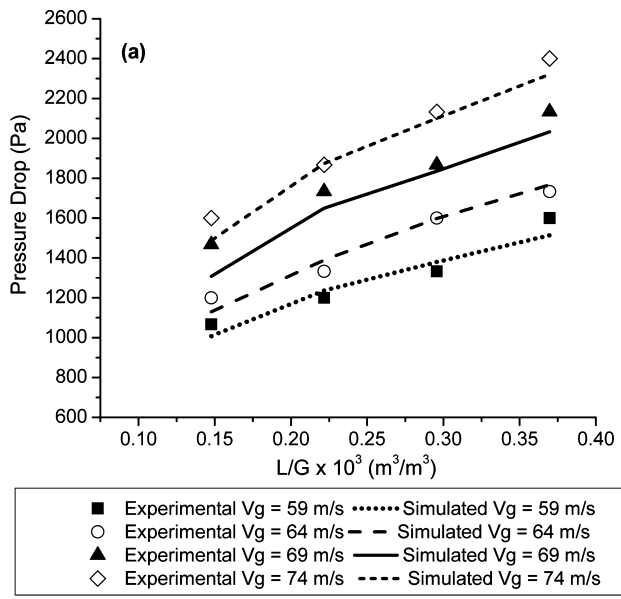
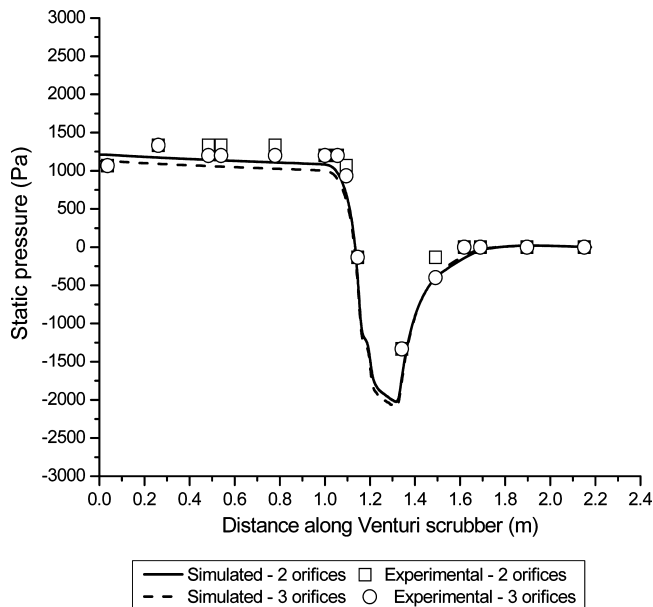


Figure 7. Effect of the velocity of gas on pressure drop (a) liquid injection through three orifices and (b) liquid injection through two orifices.

tubes in both the simulated and experimental results. In the convergent section, gas acceleration is obtained by transforming energy under the form of pressure into kinetic energy. In the throat, the gas reaches its maximum velocity and the pressure continues to drop, due to friction of the highest gas velocity with the equipment walls, but not at the same rate as in the convergence. In the diffusor, the inverse occurs: the gas loses

Figure 8. Experimental and simulated results of static pressure along the Venturi scrubber, $V_g = 64 \text{ m/s}$ and $Q_l = 1 \times 10^{-5} \text{ m}^3/\text{s}$ (two orifices, $I^{**}/D_h = 0.3$ and three orifices, $I = 0.2$).

velocity and recovers some pressure. However, because of the viscous and turbulent dissipations, not all the kinetic energy acquired at the entry of the throat returns to the diffusor in the form of pressure. Thus, the static pressure at the equipment exit is lower than at the entry, and the loss of pressure in the Venturi scrubber is the difference between the pressures measured at the entry and exit points of the equipment.

The experimental and simulated results for static pressure in a Venturi duct without liquid show insignificant deviations as can be seen in Table 1. The lowest deviation was obtained for the lowest gas velocity. Through experimental and simulated data one can verify that an increase of 25% in gas velocity in the throat of the scrubber (from 59 m/s to 74 m/s) caused an increase of 34% in the pressure drop.

4.2. Effect of Liquid Injection on the Pressure Drop of the System. Figure 4 compares the experimental and simulated static pressure profile without liquid injection to profiles with a liquid injection of $1.76 \times 10^{-5} \text{ m}^3/\text{s}$ (corresponding to a jet velocity of 7.5 m/s in each of the 3 orifices used). In both cases, the difference between the experimental and the simulated results was small. Comparing the pressure drop with and without liquid, one can observe that the value almost doubled when liquid is injected, because a greater amount of energy is required to atomize and transport the liquid.

Azzopardi and Govan²⁹ identified the mechanisms that cause the pressure drop in Venturi scrubbers: acceleration of the gas; accelerations of the droplets; acceleration of the liquid film that is deposited on the equipment walls, and friction. The importance

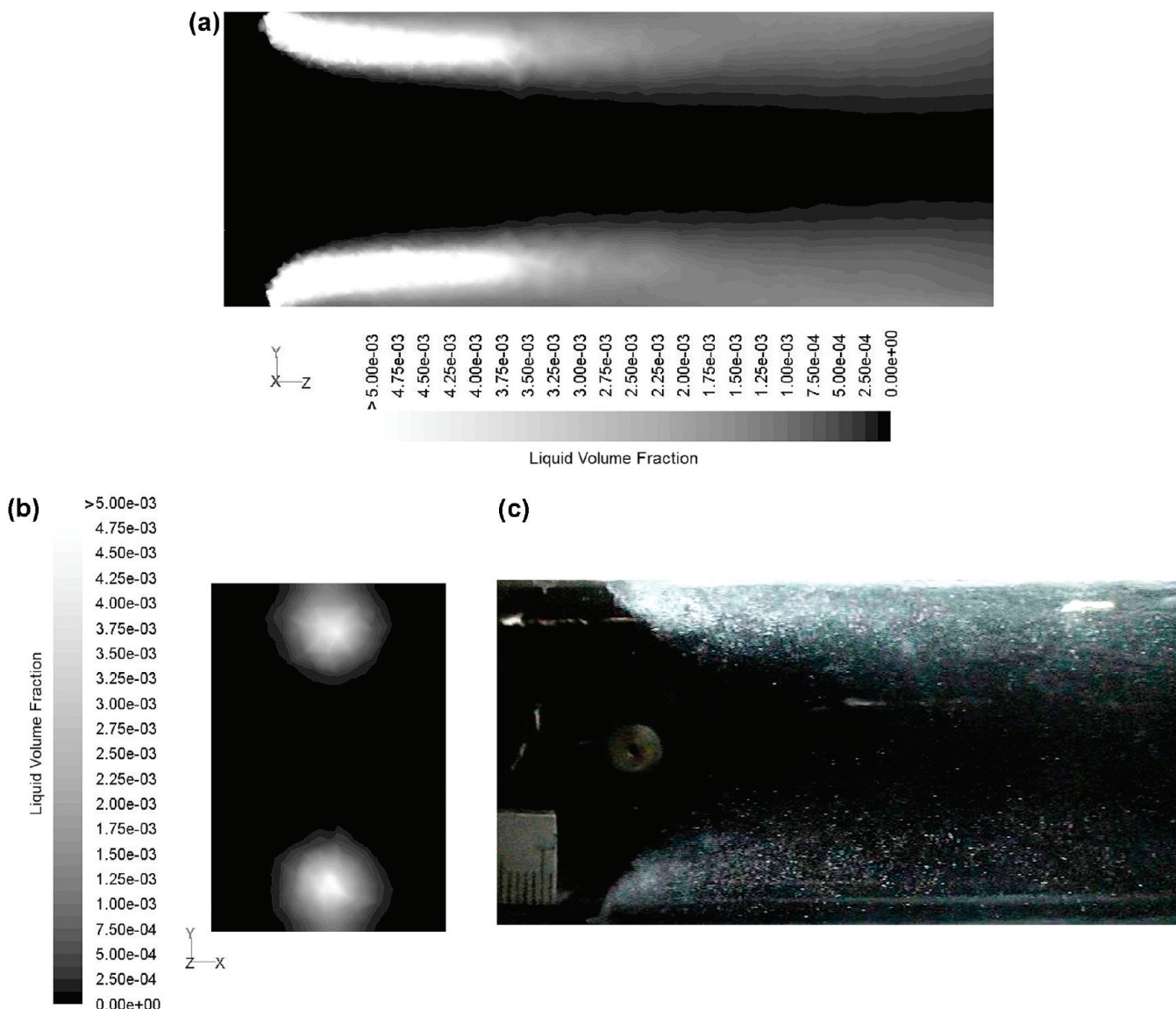


Figure 9. Liquid dispersion into gaseous phase for two orifices of liquid injection, $V_g = 64 \text{ m/s}$, $V_l = 6.5 \text{ m/s}$, $l^{**}/D_h = 0.3$: (a) simulated results of liquid volume fraction (view of the lateral plane ($y-z$)); (b) simulated results of liquid volume fraction (view of the front plane ($y-x$) located 0.035 m from the injection point); and (c) experimental image (view of the lateral plane).

of each of these mechanisms for the total pressure drop depends on the operational situation. According to Azzopardi and Govan,²⁹ in many situations of practical interest, the mechanism related to the acceleration of the liquid represents 50% to 85% of the pressure drop in the equipment.

The pressure drop in the equipment depends on the liquid flow rate, as can be seen in Figures 5a and 5b. The observable increase of the pressure drop with the increase of the liquid flow rate is expected because a higher liquid flow rate means that more energy is needed to accelerate the liquid. However, this consumption of energy depends not only on the total liquid but also on how this liquid is fractioned into droplets and how the film adhered to the walls (as well as the droplet size). These two factors depend on relative jet penetration.^{20,30} Jet velocity, the number of injection orifices, and the liquid flow rate are related, in the sense that if two of these three variables are fixed, the third one can be calculated. In most studies on Venturi scrubbers, the number of injection orifices is kept constant, and the results are studied as a

function of the liquid flow rate only. In the present study, the number of injection orifices was allowed to vary, which makes it possible to study the influence of the jet velocity (and, thus, jet penetration) while maintaining the liquid flow rate constant. Figures 6a and 6b show the variations in pressure (ΔP) for various liquid jet velocities for different numbers of liquid injection orifices, keeping the superficial gas velocity constant in the throat. As can be seen in Figures 5 and 6, the results obtained by the numerical simulation satisfactorily describe the increase in the pressure drop with the variations of both liquid flow rate and jet velocity. Tables 2 and 3 present the values of the simulated and experimental pressure drop for gas velocity (64 and 74 m/s, respectively), and the tables show that the experimental and simulated values present deviations between 1% and 10%, depending on the operating conditions.

The good agreement between the values for pressure drop, both simulated and experimental, suggests that the VOF multiphase model is capable of predicting the pressure drop in Venturi

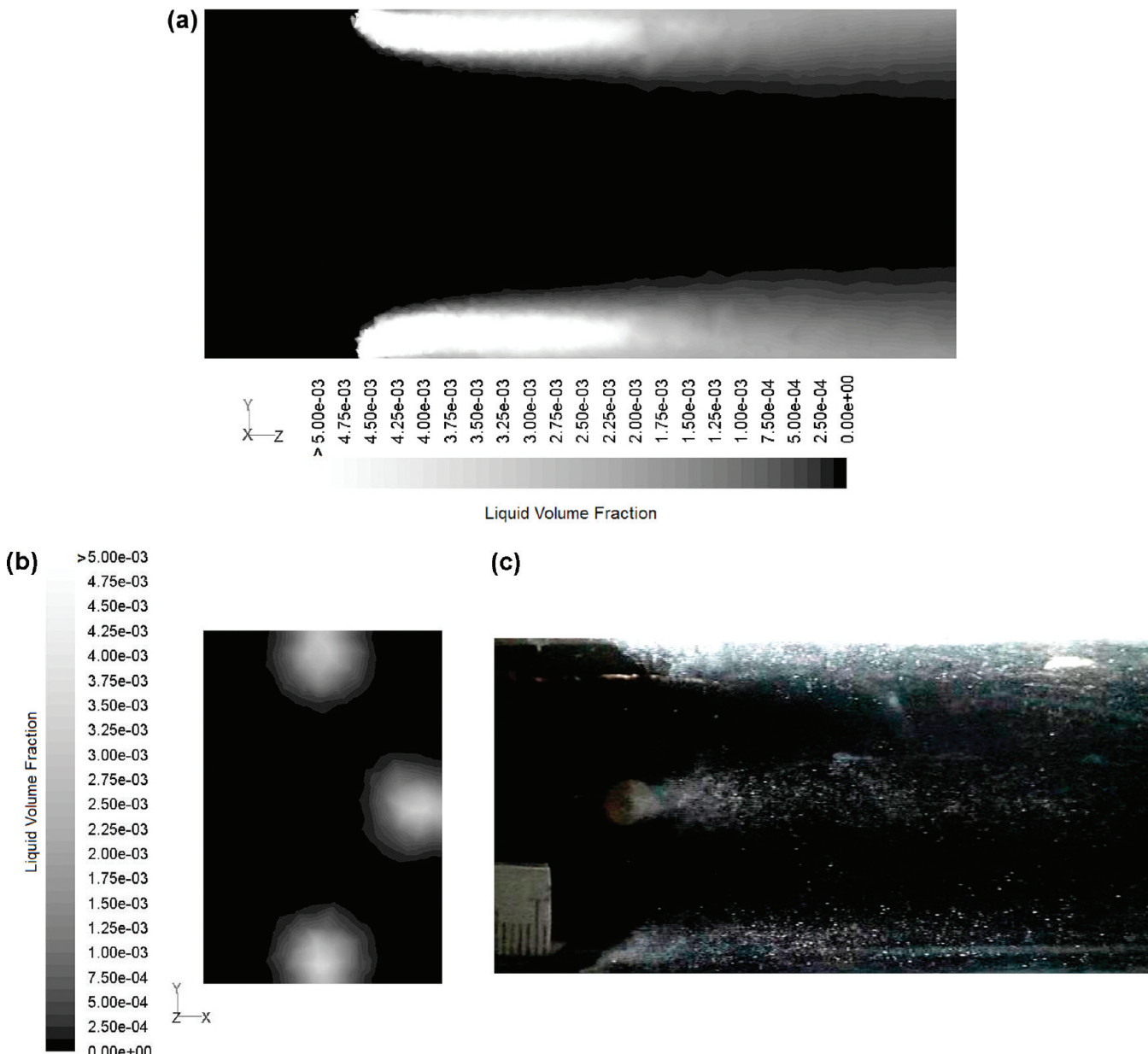


Figure 10. Liquid dispersion into gaseous phase for three orifices of liquid injection, $V_g = 64 \text{ m/s}$, $V_l = 4.3 \text{ m/s}$ and $l^{**}/D_h = 0.2$: (a) simulated results of liquid volume fraction (view of the lateral plane ($y-z$)); (b) simulated results of liquid volume fraction (view of the front plane ($y-x$) located 0.035 m from the injection point); and (c) experimental image (view of the lateral plane).

scrubbers well, even though this method does not contemplate the atomization of the liquid (that is, the breakup of the liquid into droplets of different sizes and the formation of the liquid film on the equipment walls, formed by the deposition of part of the droplets generated by the atomization). According to Viswanathan et al.,³¹ the formation of film is an important parameter that affects the pressure drop in Venturi scrubbers, causing greater pressure drop. This increase is associated to the momentum exchange of the liquid film and the formation of waves on the surface that are responsible for greater friction with the gas.^{2,29}

Figure 7 shows the influence of the gas velocity on the pressure drop for different liquid injection orifice configurations. Figures 7a and 7b show that the higher the gas velocity, the greater the pressure drop. This behavior agrees with the results reported in the literature.^{2,14,20,32} The higher the gas velocity, the greater will

be the momentum exchange and dissipation of energy through friction. The increase in gas velocity from 59 to 74 m/s caused an increase of approximately 35% in the pressure drop, independently of the configuration of the liquid injection.

To assess the influence of different injection orifice configurations on the scrubber pressure drop, the static pressure profile was plotted for the same total liquid flow rate and different numbers of injection orifices. Figure 8 shows that the number of liquid injections has little influence on the pressure drop in the equipment. However, it has a significant influence on the liquid distribution inside of the equipment as can be seen in Figures 9 and 11. Studies by Roberts and Hill³³ and Lehner³ varying the location of the injection orifices planes (or levels) showed that the pressure drop in Venturi scrubbers varies slightly by varying the position of the injection orifice planes. According to Roberts and Hill,³³ liquid injections located in the convergent section

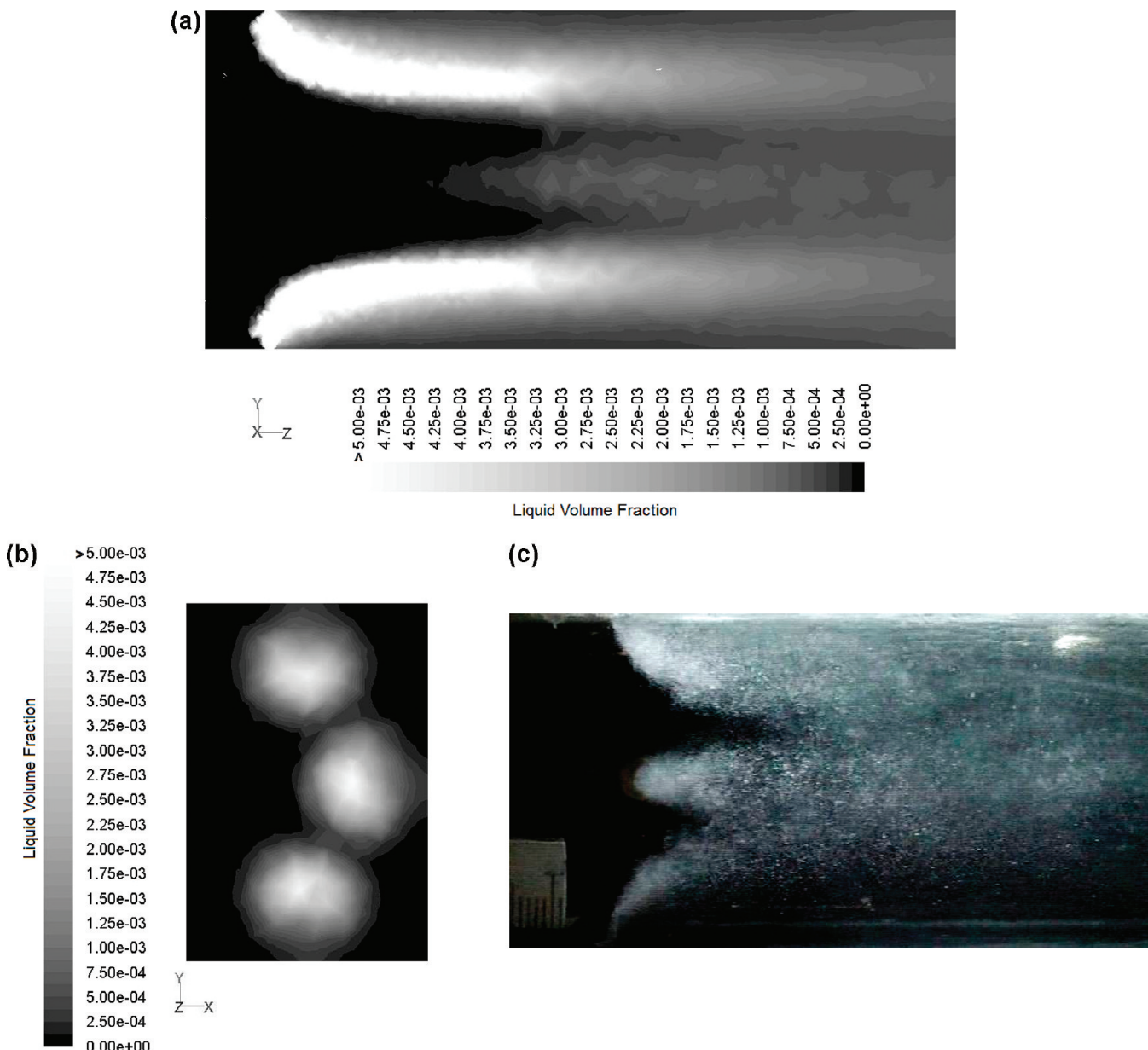


Figure 11. Liquid dispersion into gaseous phase for three orifices of liquid injection, $V_g = 64$ m/s, $V_l = 10.8$ m/s and $l^{**}/D_h = 0.5$: (a) simulated results of liquid volume fraction (view of the lateral plane ($y-z$)); (b) simulated results of liquid volume fraction (view of the front plane ($y-x$) located 0.035 m from the injection point); and (c) experimental image (view of the lateral plane).

further away from the throat are associated with lower pressure drop due to the greater flow areas and lower air velocity. In the present study, all the orifices were distributed on the same transversal plane at the equipment throat.

The majority of models available in the literature for predicting pressure drop in Venturi scrubbers do not take into consideration important factors such as convergence and divergence angles and the position of the liquid injectors. In this context, CFD simulations can contribute significantly to a more rigorous analysis of the design and performance of these gas cleaners under different conditions.

4.3. Liquid Distribution in the Venturi Scrubber Throat Using the VOF Model. Liquid distribution in the throat of the scrubber was also studied both experimentally and through CFD simulations. Simulated results of the liquid-phase volumetric fraction are presented for two planes inside the throat, one

parallel to the gas flow and cutting the throat in the middle (referred to as the “parallel view”) and another perpendicular to the gas stream and located 0.035 m downstream from the injection plane (referred to as the “frontal view”). The results are shown in Figures 9–13. Each figure shows experimental and simulated results for a given operational condition and consists of three subpictures, showing, respectively, (a) the simulated results of the liquid phase fraction on the parallel plane; (b) the simulated results for the frontal plane; and (c) the photographic image of a parallel view of the throat. The photographs include the droplets captured in the depth of the field (opposed to the simulated results, which are shown for a single plane only). It is also worth noting that the liquid on the top part of the photographs seems more dense (whiter) than the liquid on the bottom part. This is simply due to the fact that the flash made of LEDs was placed on the top of the throat.

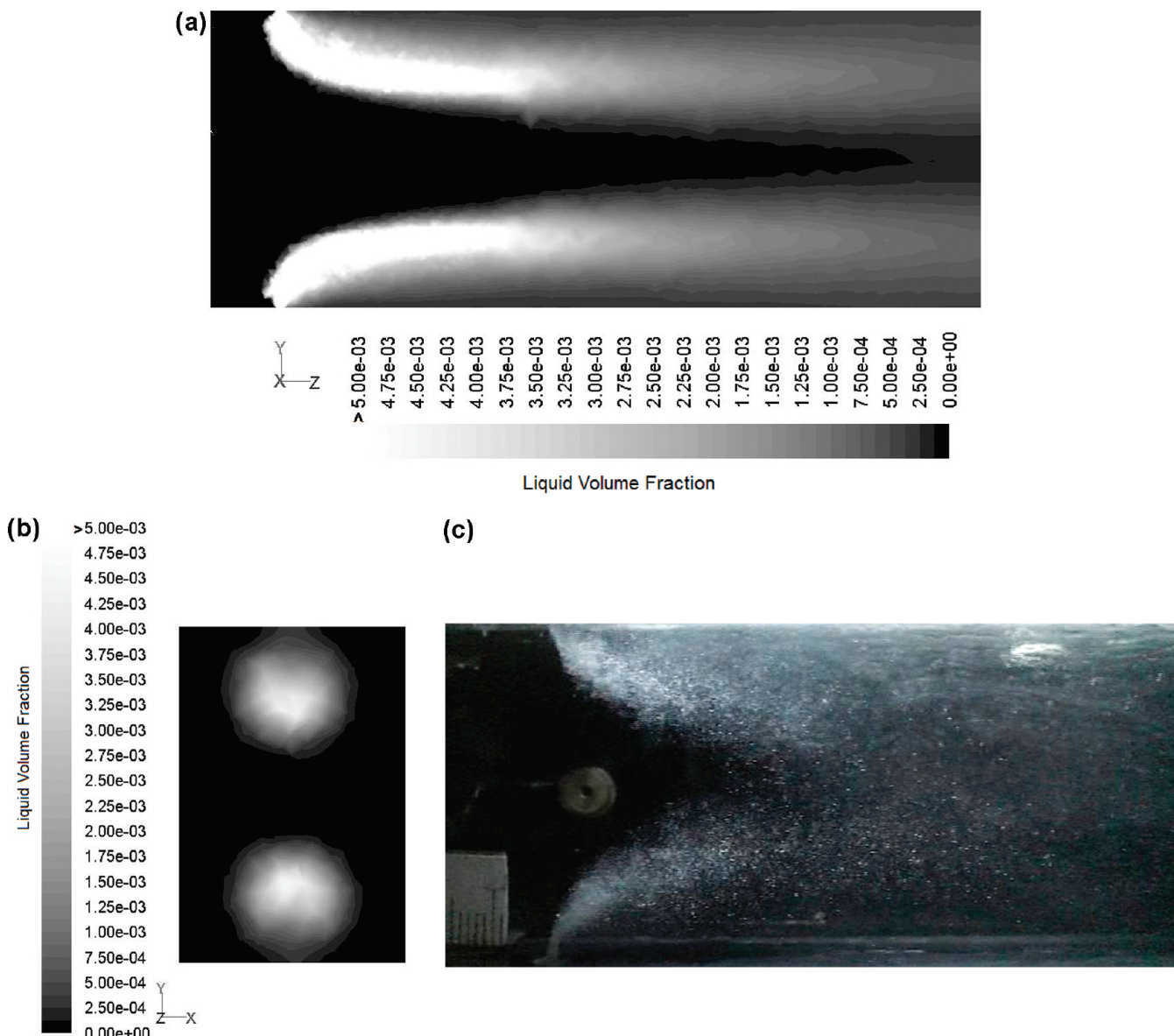


Figure 12. Liquid dispersion into gaseous phase for two orifices of liquid injection ($V_g = 59$ m/s, $V_l = 10$ m/s and $I^{**}/D_h = 0.5$): (a) simulated results of liquid volume fraction (view of the lateral plane ($y-z$)); (b) simulated results of liquid volume fraction (view of the front plane ($y-x$)) located 0.035 m from the injection point); and (c) experimental image (view of the lateral plane).

Figure 9a shows the distribution of the liquid-phase concentration on the parallel plane for a gas velocity of 64 m/s and a liquid jet velocity of 6.5 m/s, with injection through two orifices (the upper and lower orifices). Figure 9c presents a picture taken of the throat under the same operational conditions. Qualitative comparisons of the two images reveal that the distributions are qualitatively similar. In general, the initial liquid distributions obtained by the simulator using the VOF model displayed a qualitative agreement with the photographic evidence. The model was able to predict the curvature of the liquid injected through the orifices as a result of the drag forces on the body of the jet. These results indicated that VOF model can contribute to the understanding of the liquid distribution in the Venturi scrubber.

Figure 10a shows the liquid distribution on the parallel plane when the injections were made through all three orifices. However, it is not possible to see liquid emerging from the rear orifice, which indicates that the injection stream emerging from

this orifice does not penetrate long enough to reach the center of the throat. It should be emphasized that the simulated images do not make it possible to see in-depth, differently from the photograph. However, with increased jet velocity and the consequent increase in the penetration of the jets, reaching the central plane of the throat, it becomes possible to see the liquid injected through the orifice located on the wall behind the parallel plane view, as shown in Figure 11a.

The figures on liquid distribution inside the equipment, simulated as well as experimental, confirm that a higher jet velocity causes a higher jet penetration. Comparing Figures 10 and 11, which have the same number of liquid orifices injection, the increase of liquid velocity from 4.3 m/s to 10.8 m/s results in the liquid to be dispersed into the central region of the throat. Decreasing the number of liquid injection orifices for a same liquid flow rate also results in jets more penetrating in the Venturi throat. This situation can be assessed by comparing Figures 9 and 10, which show the same flow of liquid injection

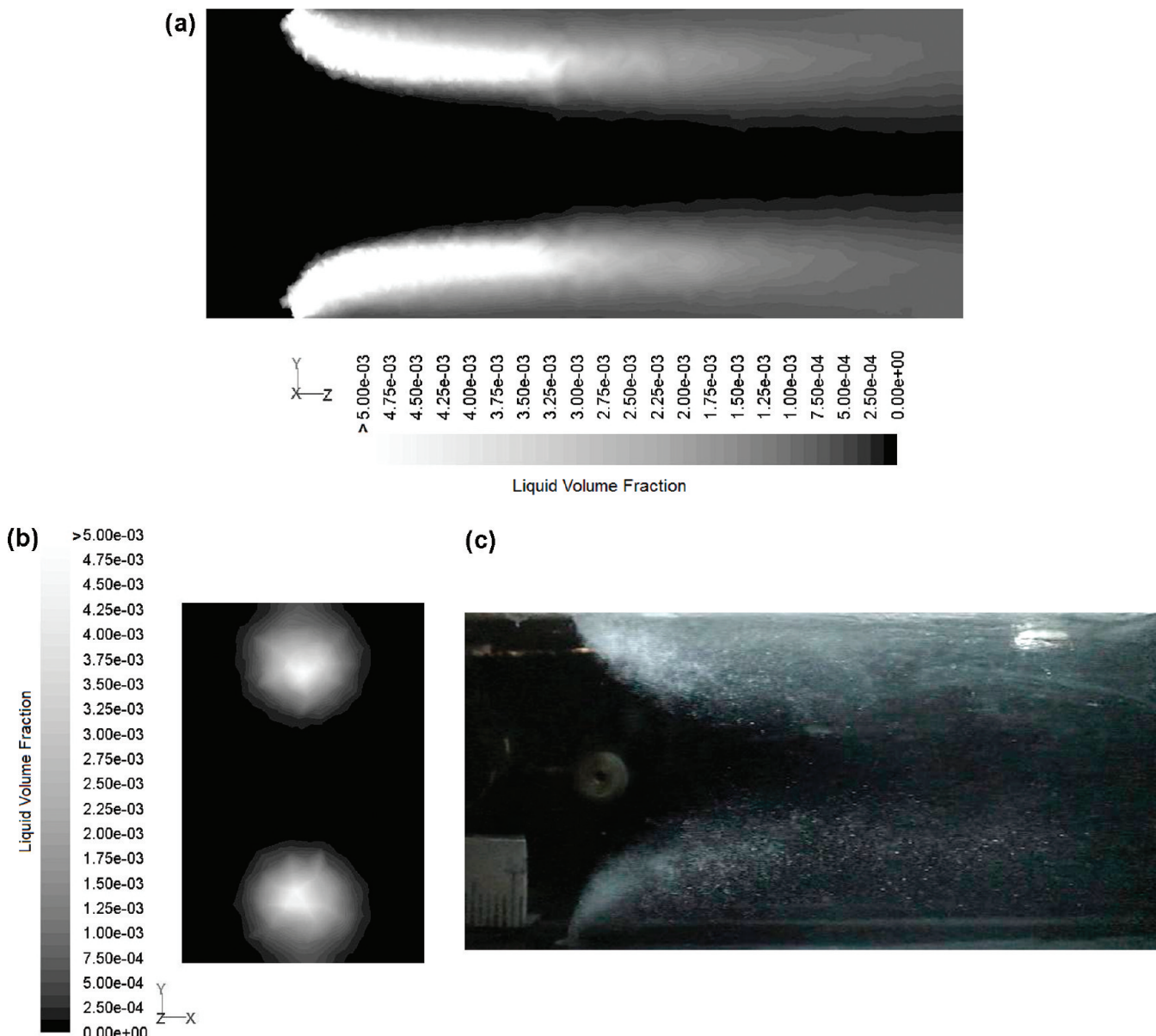


Figure 13. Liquid dispersion into gaseous phase for two orifices of liquid injection, $V_g = 74 \text{ m/s}$, $V_l = 10 \text{ m/s}$ and $I^{**}/D_h = 0.4$: (a) simulated results of liquid volume fraction (view of the lateral plane ($y-z$)); (b) simulated results of liquid volume fraction (view of the front plane ($y-x$) located 0.035 m from the injection point); and (c) experimental image (view of the lateral plane).

($Q_l = 1.0 \times 10^{-5} \text{ m}^3/\text{s}$) and different numbers of orifices. In Figure 10, it can be seen that the liquid is more concentrated around the equipment walls, because of lower jet penetration. Thus, although the number of liquid injection orifices did not affect the total pressure drop of the system significantly, it did influence the profile of liquid distribution within the equipment, which can potentially have a great impact on particle collection efficiency.

The gas velocity increase also results in jet penetration changes and consequently it can alter the liquid distribution. The model can also predict this behavior. A comparison between Figure 12 and Figure 13 shows that the increase in gas velocity from 59 m/s to 74 m/s produces a greater flattening (smaller penetration) of the liquid jet. This is caused by the increase of the drag force as a consequence of the increase in the relative velocity between the two phases, generating jets that are less penetrating for the same liquid flow rate.

5. CONCLUSIONS

- The VOF (volume of fluid) model utilized in this study was able to reproduce, within 10% of the experimental values, the pressure profiles and the pressure drop in the Venturi scrubber.
- The VOF model produced a qualitatively coherent representation of the jet curvature.
- For the same liquid flow rate, the number of injection orifices did not show significant influence on the pressure drop.
- The experimental data and simulated model confirm that the dispersion of the liquid in the scrubber throat depends strongly on the jet penetration and the configuration of the liquid injection orifices.

■ AUTHOR INFORMATION

Corresponding Author

*Tel.: +55 (16) 33518045. Fax: +55 (16) 33518266. E-mail: jasgon@ufscar.br.

Notes

The authors declare no competing financial interest.

NOMENCLATURE

A_{th} = throat area (m^2)

d_o = diameter of the liquid injection orifice (m)

D_h = hydraulic diameter of the Venturi scrubber throat (m)

l^{**} = penetration of the jet (m)

L/G = ratio of liquid flow to gas flow (L/m^3)

N_o = number of orifices for liquid injection (-)

Q_g = volumetric gas flow rate (m^3/s)

Q_l = volumetric liquid flow rate (m^3/s)

t = time (s)

V_g = gas surface velocity in the Venturi scrubber throat (m/s)

V_l = velocity of liquid injection (m/s)

v_l = velocity of the liquid phase (m/s)

α_l = volumetric fraction of the liquid phase (-)

ρ_g = gas density (kg/m^3)

ρ_l = liquid density (kg/m^3)

REFERENCES

- (1) Gonçalves, J. A. S.; Costa, M. A. M.; Henrique, P. R.; Coury, J. R. Atomization of liquids in a Pease Antony Venturi scrubber—Part II. Droplet dispersion. *J. Hazard. Mater.* **2004**, *B116*, 147.
- (2) Gonçalves, J. A. S.; Alonso, D. F.; Costa, M. A.; Azzopardi, B. J.; Coury, J. R. Evaluation of the models available for the prediction of pressure drop in Venturi scrubbers. *J. Hazard. Mater.* **2001**, *B81*, 123.
- (3) Pak, S. I.; Chang, K. S. Performance estimation of a Venturi scrubber using a computational model for capturing dust particles with liquid spray. *J. Hazard. Mater.* **2006**, *B138*, 573.
- (4) Ahmadvand, F.; Talaie, M. R. CFD modeling of droplet dispersion in a Venturi scrubber. *Chem. Eng. J.* **2010**, *160*, 423.
- (5) Bétttega, R.; Correa, R. G.; Freire, J. T. Three-Dimensional Numerical Simulation of Semi-Cylindrical and Cylindrical Spouted Bed Hydrodynamics. *Dry. Technol.* **2010**, *28*, 1266.
- (6) Bétttega, Rodrigo; Rosa, C. A.; Côrrea, R. G.; Freire, J. T. Fluid Dynamic Study of a Semi-cylindrical Spouted Bed: Evaluation of the Shear Stress Effects in the Flat Wall Region Using CFD. *Ind. Eng. Chem. Res.* **2009**, *48*, 11181.
- (7) Bétttega, R.; Correa, R. G.; Freire, J. T. Scale-up Study of Spouted Beds Using Computational Fluid Dynamics. *Can. J. Chem. Eng.* **2009**, *87*, 193.
- (8) Calvert, S. Source control by liquid scrubbing. In *Air Pollution*, 2nd ed.; Academic Press: New York, 1968; Vol. II.
- (9) Ananthanarayanan, N. V.; Viswanathan, S. Effect of nozzle arrangement on Venturi scrubber performance. *Ind. Eng. Chem. Res.* **1999**, *38*, 4889.
- (10) Boll, R. H. Particle collection and pressure drop in Venturi scrubbers. *Ind. Eng. Chem. Fund.* **1973**, *12*, 40.
- (11) Yung, S. C.; Barbarika, H. F.; Calvert, S. Pressure loss in Venturi scrubbers. *J. Air Pollut. Control Assoc.* **1977**, *27*, 348.
- (12) Leith, D.; Martin, K. P.; Cooper, D. W. Liquid utilisation in a Venturi scrubber. *Filtr. Separat.* **1985**, May/June, 191.
- (13) Viswanathan, S.; Gnyp, A. W.; St. Pierre, C. Annular flow pressure drop model for Pease–Antony type Venturi scrubbers. *AIChE J.* **1985**, *31*, 1947.
- (14) Azzopardi, B. J.; Teixeira, S. F. C. F.; Govan, A. H.; Bott, T. R. An improved model for pressure drop in Venturi scrubbers. *Trans. Inst. Chem. Eng.* **1991**, *69*, 55.
- (15) Sun, H.; Azzopardi, B. J. Modeling gas–liquid flow in Venturi scrubber at high pressure. *Process Saf. Environ.* **2003**, *81*, 250.
- (16) Rahimi, A; Niksiar, A.; Mobasher, M. Considering roles of heat and mass transfer for increasing the ability of pressure drop models in Venturi scrubbers. *Chem. Eng. Process.* **2011**, *50*, 104.
- (17) Ekman, F. O.; Johnstone, H. F. Collection of aerosols in a Venturi scrubber. *Ind. Eng. Chem.* **1951**, *43*, 1358.
- (18) Shyan, L. D.; Viswanathan, S. Effect of polydispersity of droplets in the prediction of flux distribution in a Venturi Scrubber. *Environ. Sci. Technol.* **2000**, *34*, 5007.
- (19) Ananthanarayanan, N. V.; Viswanathan, S. Estimating maximum removal efficiency in Venturi scrubbers. *AIChE J.* **1998**, *44*, 2549f.
- (20) Guerra, V. G.; Gonçalves, J. A. S.; Coury, J. R. Experimental investigation on the effect of liquid injection by multiple orifices in the formation of droplets in a Venturi scrubber. *J. Hazard. Mater.* **2009**, *161*, 351.
- (21) Lehner, M. Aerosol Separation Efficiency of a Venturi scrubber working in self-priming mode. *Aerosol Sci. Technol.* **1998**, *28*, 389.
- (22) Delteil, J.; Vincent, S.; Erriquible, A.; Subra-Paternault, P. Numerical investigations in Rayleigh breakup of round jets with VOF methods. *Comput. Fluids* **2011**, *50*, 10.
- (23) Viswanathan, S.; ST. Pierre, C.; Gnyp, A. W. Jet penetration measurements in a Venturi scrubber. *Can. J. Chem. Eng.* **1983**, *61*, 504.
- (24) Puentes, N. A. G.; Guerra, V. G.; Coury, J. R.; Gonçalves, J. A. S. Droplet dispersion angle measurements on a Pease-Antony Venturi scrubber. *Braz. J. Chem. Eng.* **2012**, *29*, 99.
- (25) Hirt, C. W.; Nichols, B. D. Volume of Fluid (VOF) Method for the dynamics of free boundaries. *J. Comput. Phys.* **1981**, *39*, 201.
- (26) FLUENT 12.0 Theory Guide; Fluent, Inc.: Lebanon, NH, 2009.
- (27) Orszag, S. A.; Yakhot, V.; Flannery, W. S.; Boysan, F.; Choudhury D.; Maruzewski, J.; Patel, B. Renormalization group modeling and turbulence simulations. Presented at the *International Conference on Near-Wall Turbulent Flows*, Tempe, AZ, March 1993; Paper No. 1031.
- (28) FLUENT 12.0 User's Guide, Chapter 26; Fluent, Inc.: Lebanon, NH, 2009.
- (29) Azzopardi, B. J.; Govan, A. H. The modeling of Venturi scrubbers. *Filtr. Separat.* **1984**, *21*, 196.
- (30) Guerra, V. G.; Gonçalves, J. A. S.; Coury, J. R. Experimental verification of the effect of liquid deposition on droplet size measured in a rectangular Venturi scrubber. *Chem. Eng. Process* **2011**, *50*, 1137.
- (31) Viswanathan, S. Examination of liquid film characteristics in the prediction of pressure drop in a Venturi scrubber. *Chem. Eng. Sci.* **1998**, *53*, 3161.
- (32) Leith, D.; Cooper, D. W. Venturi scrubber optimization. *Atmos. Environ.* **1980**, *14*, 657.
- (33) Roberts, D. B.; Hill, J. C. Atomization in a Venturi Scrubber. *Chem. Eng. Commun.* **1981**, *12*, 33.